

theoretical curves are calculated from the RC constants. A 1.02-mm-long modulator showed a 3 dB bandwidth of 5.4 GHz and a driving voltage of 2.1 V to obtain a transmission change from 90% to 10% and 5.5 V for 20 dB extinction ratio, at 5.4 mW input power and $\Delta E_g = 50$ meV. Moreover, the theoretical curves tell us that we can obtain a 10 GHz-bandwidth modulator when ΔE_g is 50 meV, the stripe width is 2 μm and the device length is about 950 μm .

Fig. 3a shows a detected eye pattern for a 5 Gbit/s NRZ pseudorandom pulse with the modulation voltage of 4 V. The extinction ratio was about 20 dB and the eye was clearly opened, even at 5.4 mW input optical power.

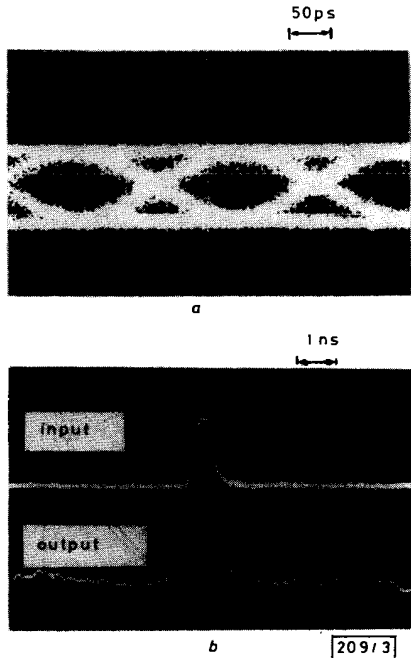


Fig. 3

a Eye pattern for 5 Gbit/s NRZ pseudorandom pulse modulation at 5.4 mW input optical power. Modulation voltage is 4 V and extinction ratio is 20 dB

b 100 km single-mode fibre transmission. Upper trace is input waveform and lower trace is transmitted one. Dispersion of fibre is 17 ps/km/nm and α -parameter of modulator is 1.2

A 100 km optical pulse transmission experiment has been achieved using a conventional single-mode fibre. The fibre dispersion at 1.55 μm , the wavelength of the incident light, was 17 ps/km/nm. Fig. 3b shows waveforms of an input pulse and its transmitted pulse. The spread of the pulse width was small, i.e. from 530 ps to 550 ps, and the waveform was well preserved. The observed spread of about 20 ps is reasonable when we consider the fibre dispersion and the linewidth enhancement factor α of 1.2 of the used modulator identified by the spectral measurement method.¹

Conclusion: GaInAsP electroabsorption modulators were studied from a viewpoint of milliwatt range output operation. It was found that the degradation of the bandwidth due to high input optical power was strongly dependent on ΔE_g , i.e. the absorption coefficient. However, the degradation was as small as 1 dB or less if ΔE_g was over 50 meV, even under several mW input power. Experimental results showed that low driving voltage and high-speed modulation were compatibly achieved under the milliwatt range output power condition, and a 100 km single-mode fibre pulse transmission experiment succeeded.

Acknowledgment: We thank Dr. Y. Kushiuro, Dr. K. Sakai, Dr. Y. Matsushima, Dr. Y. Noda, Dr. K. Utaka and Mr. M. Usami of KDD Meguro R&D Laboratories for their fruitful

discussions, and Mr. N. Edagawa for his help in experiments. We also acknowledge Dr. T. Muratani and Dr. T. Yamamoto of KDD for their continuous encouragement.

M. SUZUKI
H. TANAKA
S. AKIBA

3rd August 1988

KDD Meguro R&D Laboratories
2-1-23 Nakameguro
Meguro-ku, Tokyo 153, Japan

References

- 1 NODA, Y., SUZUKI, M., KUSHIRO, Y., and AKIBA, S.: 'High-speed electroabsorption modulator with strip-loaded GaInAsP planar waveguide', *J. Lightwave Technol.*, 1986, LT-4, pp. 1445-1453
- 2 WOOD, T. H.: 'Multiple quantum well (MQW) waveguide modulators', *ibid.*, 1988, LT-6, pp. 743-757
- 3 KOREN, U., MILLER, B. I., KOCH, T. L., EISENSTEIN, G., TUCKER, R. S., BAR-JOSEPH, I., and CHEMLA, D. S.: 'Low-loss InGaAs/InP multiple quantum well optical electroabsorption waveguide modulator', *Appl. Phys. Lett.*, 1987, 51, pp. 1132-1134

SCALING 'BALLISTIC' HETEROJUNCTION BIPOLAR TRANSISTORS

Indexing terms: Semiconductor devices and materials, Bipolar devices, Transistors

Reducing length scales in npn heterojunction bipolar transistors leads to unexpected changes in the fundamental limits of device performance. Very high p-type carrier concentrations in the base result in a reduced inelastic electron scattering rate. In addition, there exists a maximum base/collector bias above which ballistic collector transport is not possible, and correct scaling requires the n-type collector contact to be unusually heavily doped.

Fig. 1 shows a schematic band diagram of an npn heterojunction bipolar transistor (HBT) with base width Z_b and collector transit region width Z_c . Recently it was shown that

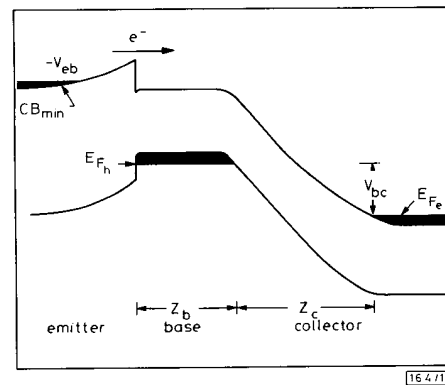


Fig. 1 Schematic band diagram of npn HBT under bias

Base width Z_b , collector transit region width Z_c , conduction band minimum CB_{min} and electron (hole) quasi-Fermi level E_{Fn} (E_{Fp}) are indicated

extreme nonequilibrium electron transport in the base of an AlGaAs/GaAs HBT is possible when the base width Z_b is similar to the mean free path λ of charge carriers injected from the emitter.¹ In this case inelastic scattering of conduction band electrons with the coupled excitations of the p-type majority carriers/optical phonons in the base determines the value of λ . It has also been shown that Γ -X intervalley scattering is significant for large collector transit region widths

($Z_c \gtrsim 1000 \text{ \AA}$), but becomes much less important for $Z_c \lesssim 500 \text{ \AA}$.² Obviously, if one wishes to take advantage of hot carrier effects and improve the performance of HBTs, it is necessary to understand what happens when Z_b and Z_c are reduced in length. The purpose of this letter is to illustrate how scaling can lead to unexpected changes in fundamental limits of device performance set by the emitter-collector transit time. (Note that for the present discussion it is assumed that, as in $\text{InP/Ga}_{0.47}\text{In}_{0.53}\text{As}$ HBTs, device area can be scaled with Z_c without, for example, adversely altering the transistor's current gain.³)

A reduction in Z_b requires an increase in p , the majority charge carrier density in the base, to keep the base sheet resistance $R_{b\Box}$ acceptably small. For example, GaAs with a p -type carrier concentration of $p = 2 \times 10^{20} \text{ cm}^{-3}$ has a mobility $\mu \approx 50 \text{ cm}^2 \text{ V}^{-1} \text{ s}^{-1}$,⁴ so that a sheet resistance of $R_{b\Box} \lesssim 200 \Omega_{\Box}$ requires $Z_b \gtrsim 300 \text{ \AA}$. Now consider the effect these parameters have on nonequilibrium electron transport in the base. A conduction band electron of energy E_i above the conduction band minimum CB_{\min} is injected into the p -type base. This electron may scatter inelastically, losing energy $Y = \hbar\omega/E_{F_h}$ and changing momentum by $X = q/k_{F_1}$, where E_{F_h} is the Fermi energy of the majority p -type carriers in the base and k_{F_1} is the Fermi wave vector of the heavy-hole band. To calculate the total inelastic scattering rate $1/\tau_{in}$ for a fixed injection energy E_i (see Reference 5), we need to integrate over the spectral weight in the dispersion relation for the coupled majority carrier/optical phonon system in p -type GaAs. Within effective mass theory energy and momentum conservation results in a parabola of integration which, for the indicated p -type carrier concentrations, leads to the broken lines plotted in Fig. 2. Calculation of $1/\tau_{in}$ requires integration

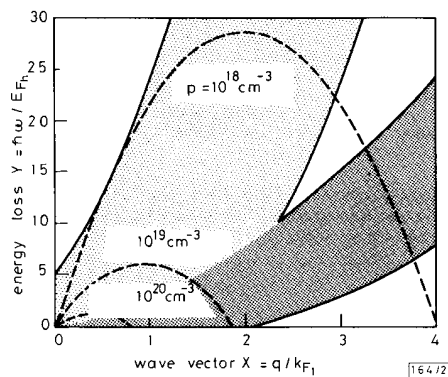


Fig. 2 Dispersion relation for single particle excitations in p -type GaAs. Broken lines are parabolas of integration for three different p -type carrier concentrations and for conduction band electron injection energy $E_i = 200 \text{ meV}$

of the spectral weight within the parabola. It is clear from the Figure that small values of p involve an integration over a large portion of the heavy-hole interband single particle excitations (dark shaded region in Fig. 2), which carry most of the inelastic scattering strength. With increasing p a reduced portion of phase space is integrated. Although, for large values of p , total scattering strength increases, over the small region of phase space in which the integration takes place the scattering strength can decrease. A consequence of this is that, with increasing carrier concentration, $1/\tau_{in}$ increases, reaches a maximum and then decreases. This fact is illustrated in Fig. 3a, in which results of calculating $1/\tau_{in}$ for GaAs as a function of p are given for three different values of E_i . For low values of $p \lesssim 10^{17} \text{ cm}^{-3}$ optical-phonon scattering dominates. At very high values of $p \gtrsim 5 \times 10^{20} \text{ cm}^{-3}$, $1/\tau_{in}$ is less than the bare optical-phonon scattering rate because of screening effects. Since the physics underlying the decrease in $1/\tau_{in}$ at high p is based on a phase space argument, the results are general and apply to other material systems such as $\text{Ga}_{0.47}\text{In}_{0.53}\text{As}$ and InAs .

1274

If the high carrier concentration in the base is created using randomly positioned impurities, then it is necessary to consider the elastic scattering rate due to those ionised impurities, $1/\tau_{ei}$. The results of calculating $1/\tau_{ei}$ as a function of p for three values of E_i are shown in Fig. 3b. It is clear from the

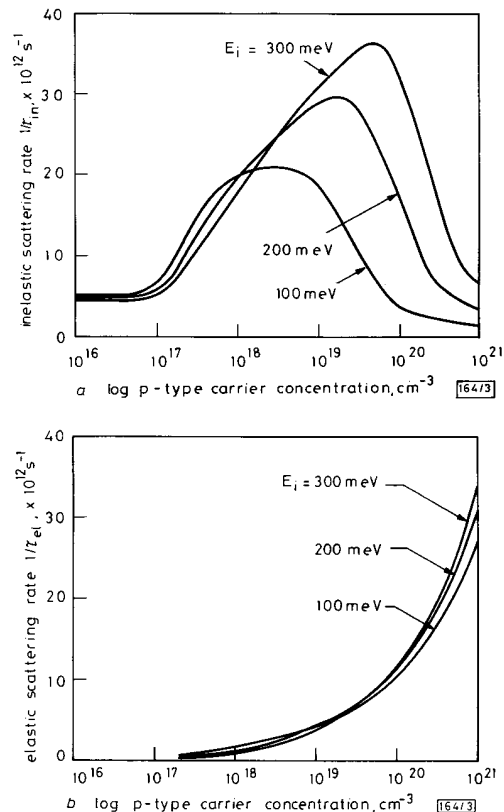


Fig. 3

a Total inelastic scattering rate $1/\tau_{in}$ as function of p -type carrier concentration in GaAs for three indicated values of electron energy E_i
b Total elastic electron scattering rate $1/\tau_{ei}$ for p -GaAs. Parameters used in calculations were effective heavy-hole mass = $0.5m_0$, light-hole mass = $0.082m_0$, conduction band effective electron mass = $0.07m_0$, high-frequency dielectric constant $\epsilon_{\infty} = 10.91$, longitudinal optical-phonon energy $\hbar\omega_{LO} = 36.5 \text{ meV}$, and transverse optical-phonon energy $\hbar\omega_{TO} = 33.8 \text{ meV}$

Figure that $1/\tau_{ei}$ is the dominant scattering process for $p \gtrsim 5 \times 10^{20} \text{ cm}^{-3}$. Rather than attempt to optimise $1/\tau_{ei}$ and $1/\tau_{in}$, it is better to eliminate the contribution from $1/\tau_{ei}$ by placing impurities in a periodic sublattice either by atomic layer epitaxy techniques such as delta doping⁶ or by creating new ordered semiconductor alloys.⁷

We now consider fundamental limits to collector transport. For $Z_c \lesssim 500 \text{ \AA}$ collector transit times can be so short that Γ - X intervalley transfer does not dominate collector transport dynamics.² For small Z_c the limit to ballistic collector transport depends on the base/collector bias V_{bc} and the width in energy of the conduction band, $E_{b\omega}$. In the collector arm the electron can be accelerated only to an energy $E \leq E_{b\omega}$ before interband scattering takes place. To avoid this we require $eV_{bc}^{\max} \lesssim E_{b\omega} - E_g - E_{F_s} - E_{F_p}$, where E_g is the semiconductor bandgap. Ignoring the contribution from E_{F_s} and E_{F_p} , we note that for GaAs $E_{b\omega} = 2.0 \text{ eV}$ and $E_g = 1.4 \text{ eV}$, giving $eV_{bc}^{\max} = 0.6 \text{ eV}$, and for $\text{Ga}_{0.47}\text{In}_{0.53}\text{As}$ $E_{b\omega} = 2.25 \text{ eV}$, $E_g = 0.75 \text{ eV}$ giving $eV_{bc}^{\max} = 1.5 \text{ eV}$.

The existence of extreme nonequilibrium electron transport in structures with small Z_b and Z_c give emitter-collector transit times τ_{ec} that are very short. For example, $Z_b = 300 \text{ \AA}$,

$Z_c = 500 \text{ \AA}$ and an average velocity of $8 \times 10^7 \text{ cm s}^{-1}$ gives $\tau_{ec} = 0.1 \text{ ps}$. Clearly, with such small values of τ_{ec} it is necessary to consider the temporal response of the n^+ collector contact to the arrival of a hot electron. This time is related to the dielectric response of the contact, which is approximately given by the plasma frequency $\omega_p = 2\pi/\tau_p$. As an example, in GaAs $\tau_p \approx 0.1 \text{ ps}$ for $n = 1 \times 10^{18} \text{ cm}^{-3}$, and $\tau_p \approx 0.03 \text{ ps}$ for $n = 1 \times 10^{19} \text{ cm}^{-3}$. Because we require $\tau_{ec} \gg \tau_p$ this suggests that a heavily doped n -type collector contact ($n \geq 10^{19} \text{ cm}^{-3}$) is advantageous.

In summary, scaling ballistic HBTs leads to some unexpected results. First, inelastic scattering of injected carriers in the base decreases for very high values of p -type carrier concentrations; secondly, ballistic transport in the collector arm is only possible for a base/collector bias below a critical value; and thirdly, to correctly scale the device, the collector contact must have a high n -type carrier concentration.

I thank K. Berthold and R. N. Nottenburg for useful discussions.

A. F. J. LEVI
AT&T Bell Laboratories
Murray Hill, NJ 07974, USA

29th July 1988

References

- BERTHOLD, K., LEVI, A. F. J., WALKER, J., and MALIK, R. J.: 'Extreme nonequilibrium electron transport in heterojunction bipolar transistors', *Appl. Phys. Lett.*, 1988, **52**, pp. 2247-2249
- LEVI, A. F. J., SPÄH, R. J., and ENGLISH, J. H.: 'Electron-transport dynamics in quantized intrinsic GaAs', *Phys. Rev. B.*, 1987, **36**, pp. 9402-9405
- NOTTENBURG, R. N., CHEN, Y. K., PANISH, M. B., and HUMPHREY, D. A.: 'High current gain submicrometer InGaAs/InP heterostructure bipolar transistors', *Electron Dev. Lett.*, 1988, accepted for publication
- MADELUNG, O., SCHULZ, H., and WEISS, H. (Eds.): 'Landolt-Börnstein tables' (Springer, Berlin, 1982), Vol. III/17a and References therein
- LEVI, A. F. J., and YAFET, Y.: 'Nonequilibrium electron transport in bipolar devices', *Appl. Phys. Lett.*, 1987, **51**, pp. 42-44
- SCHUBERT, E. F., CUNNINGHAM, J. E., and TSANG, W. T.: 'Realization of the Esaki-Tsu type doping superlattice', *Phys. Rev. B.*, 1987, **36**, pp. 1348-1351
- GOMYO, A., SUZUKI, T., and IJIMA, S.: 'Observation of strong ordering in $\text{Ga}_{1-x}\text{In}_x\text{P}$ alloy semiconductors', *Phys. Rev. Lett.*, 1988, **60**, pp. 2645-2648

1.3 μm GaInAsP NEAR-TRAVELLING-WAVE LASER AMPLIFIERS MADE BY COMBINATION OF ANGLED FACETS AND ANTIREFLECTION COATINGS

Indexing terms: Semiconductor lasers, Optical communications

1.3 μm GaInAsP near-travelling-wave laser amplifiers have been realised by the combination of angled facets and antireflection coatings. Without *in situ* monitoring on the device itself during dielectric coatings, we can routinely obtain a low effective modal facet reflectivity of $5\text{--}8 \times 10^{-4}$. The devices had an internal gain of $24 \pm 1.5 \text{ dB}$ for the TE mode and a single-mode fibre coupling loss of 5 dB/facet.

Introduction: The travelling-wave laser amplifier has been demonstrated as an optical repeater to compensate for the transmission loss¹ and as a preamplifier to overcome the receiver noise.² It is a very useful optical device, especially in high-bit-rate and multichannel optical fibre communication systems. Its facet reflectivity has to be low to obtain wide bandwidth and high output saturation power.³ Presently, near-travelling-wave (NTW) laser amplifiers rely solely on extremely low- ($\leq 10^{-3}$) reflectivity coatings on ordinary laser facets to prohibit the Fabry-Perot resonance. To achieve such a low facet reflectivity requires extremely tight control of the refractive indices and thicknesses of dielectric layers.^{4,5}

We have previously demonstrated a simpler way to realise 1.5 μm NTW laser amplifiers by angled facets.⁶ The Fabry-Perot resonance is suppressed only by slanting the waveguide (gain region) from the cleavage plane such that the internal light reflected by the cleaved facets does not couple back into the waveguide directly and is therefore mostly lost (Fig. 1a).

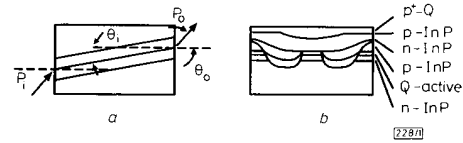


Fig. 1 Schematic drawings of NTW laser amplifier with angled facets
a Top view ($\theta_i = 7^\circ$, $\theta_o = 22^\circ$) b Cross-sectional view
For conciseness, only waveguide is shown in (a)

However, with antireflection (AR) coatings, the coupling efficiency to single-mode fibres is better. In this letter we report the performance of 1.3 μm GaInAsP NTW laser amplifiers made by the combination of angled facets and AR coatings. With the angled facet structure, AR coatings of 1-5% reflectivity are sufficient to remove the facet reflection loss as well as to further reduce the residual facet reflectivity. Such coatings are relatively easy to achieve.

Device fabrication: The NTW laser amplifiers are made from 1.3 μm GaInAsP/InP wafers grown by LPE. The double-channel planar buried heterostructure is used for current and optical confinements (Fig. 1b). The waveguide is oriented $\sim 7^\circ$ away from the [011] direction (Fig. 1a). The wafer is cleaved along the [011] direction into devices 508 μm long. Then, both facets are coated with zirconium oxide with a thickness of approximately a quarter dielectric wavelength by electron-beam evaporation. The thickness is controlled with a crystal thickness monitor, but without *in situ* monitoring on the device itself.

Device performance: Since the effective modal facet reflectivity before coating is quite low already ($\sim 0.5\%$), the light/current characteristics (Fig. 2) before and after AR coatings look like those of a superluminescent diode. By AR coating, the facet Fresnel reflection is reduced from $\sim 38\%$ to $\sim 1\%$ and the light output increases proportionally. Therefore, AR coatings ($\sim 1\%$) are helpful to reduce the coupling loss. With the same

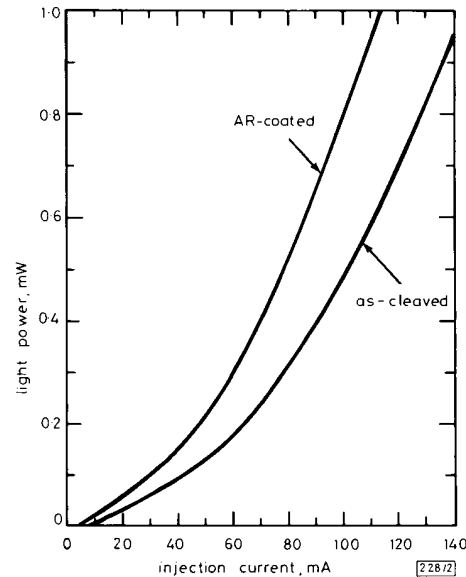


Fig. 2 Light power against injection current before and after anti-reflection coatings